Geophysical Research Letters

RESEARCH LETTER
10.1029/2019GL083951

Key Points:
- A 250,000-year record of speleothem growth from Wisconsin (USA) reveals differing permafrost persistence in the last two glacial periods
- Paleo-permafrost indicators across the American Midwest suggest that the penultimate glaciation was warmer than the last glacial period
- A network of midlatitude and tropical sea surface temperatures demonstrates a 1 °C difference between the last two glacial periods

Supporting Information:
- Supporting Information S1
- Table S1

Correspondence to:
C. J. Batchelor,
batchelor2@wisc.edu

Citation:
Batchelor, C. J., Orland, I. J., Marcott, S. A., Slaughter, R., Edwards, R. L., Zhang, P., et al. (2019). Distinct permafrost conditions across the last two glacial periods in midlatitude North America. *Geophysical Research Letters*, *46*, 13,318–13,326. https://doi.org/10.1029/2019GL083951

Received 31 MAY 2019
Accepted 25 SEP 2019
Accepted article online 15 OCT 2019
Published online 20 NOV 2019

Distinct Permafrost Conditions Across the Last Two Glacial Periods in Midlatitude North America

Cameron J. Batchelor[1], Ian J. Orland[1,2], Shaun A. Marcott[1], Richard Slaughter[1], R. Lawrence Edwards[3], Pu Zhang[3], Xianglei Li[3], and Hai Cheng[3,4]

[1]Department of Geoscience, University of Wisconsin-Madison, Madison, WI, USA, [2]Wisconsin Geological and Natural History Survey, University of Wisconsin-Madison, Madison, WI, USA, [3]Department of Earth Sciences, University of Minnesota, Minneapolis, MN, USA, [4]Institute of Global Environmental Change, Xi'an Jiatong University, Xi'an, China

Abstract During past glacial periods, extensive areas of North America were covered by permafrost. The timing and extent of these paleo-permafrost conditions, however, remains ambiguous. Here we present a 250,000-year record of speleothem growth from a midlatitude North American cave and report 141 U-Th ages with hiatuses in growth that reflect the development of temporally continuous permafrost. Combined with U-Th ages from other speleothem studies, we demonstrate that regional permafrost conditions occurred during both of the prior two glacial maxima but were markedly shorter in duration during the penultimate (Marine Isotope Stage 6, MIS 6) versus the last (MIS 2) glacial period. Notably, a network of sea surface temperatures indicates that mid- and low-latitude temperatures were 0.9 °C ± 0.2 °C warmer during the culmination of MIS 6 versus MIS 2. Our results illustrate the importance of developing regional paleo-permafrost records and highlight the sensitivity of permafrost conditions during glacial periods to relatively small differences in global-scale temperature.

Plain Language Summary Permafrost is an important reservoir of carbon during glacial periods. Our understanding of the timing and spatial extent of permafrost conditions during recent glaciations, however, is lacking because of a paucity of paleo-permafrost indicators. Here we present a new, high-precision chronology of speleothem growth in a Wisconsin (USA) cave that constrains permafrost conditions during the last two glacial periods. The new record suggests that permafrost conditions endured for 18 ka during the culmination of the last glacial period but were ephemeral during the penultimate glacial period. Our findings are supported by sea surface temperature reconstructions that indicate the penultimate glaciation was nearly 1 °C warmer than the last glacial period. These results provide useful information for quantifying the sensitivity of permafrost to past temperature changes.

1. Introduction

Throughout the Quaternary, Earth's climate has cycled between glacial and interglacial periods in response to both external (Hays et al., 1976) and internal climate forcings (Budyko, 1969; Sellers, 1969). These fluctuations had profound effects on global ice volume (Lisiecki & Raymo, 2005) and permafrost extent (Vaks et al., 2013), which in turn directly influences sea level (Shakun et al., 2015) and global carbon cycling (Zimov et al., 2006). Presently, permafrost covers approximately 23 million km^2 of land in the Northern Hemisphere, a third of which is located in North America (Figure 1a; Smith et al., 2010). As modern climate continues to warm, the environmental impacts resulting from the thawing of permafrost will be extensive, especially at high latitudes (Grosse et al., 2011). The most notable, and global, consequence could be the release of newly mobilized carbon from thawed soils, which models suggest would intensify existing warming and have far-reaching economic costs (Hope & Schaefer, 2016).

The multidecadal- to centennial-scale response of permafrost to projected future warming is obscured, however, because instrumental records of permafrost fail to capture trends longer than a few decades (Heimann & Reichstein, 2008; Zimov et al., 2006). The geologic archive provides a unique opportunity to constrain the sensitivity of permafrost to temperature changes over longer timescales. Several paleo-permafrost geomorphic features have been identified in midlatitude North America (Figure 1b; Clayton et al., 2001), suggesting permafrost conditions persisted across the landscape during the last glacial period. The dating methods (i.e., radiocarbon dating) used to fingerprint the age of these features, however, only span the last ~50,000 years, which limits our understanding of former permafrost conditions to this relatively narrow time

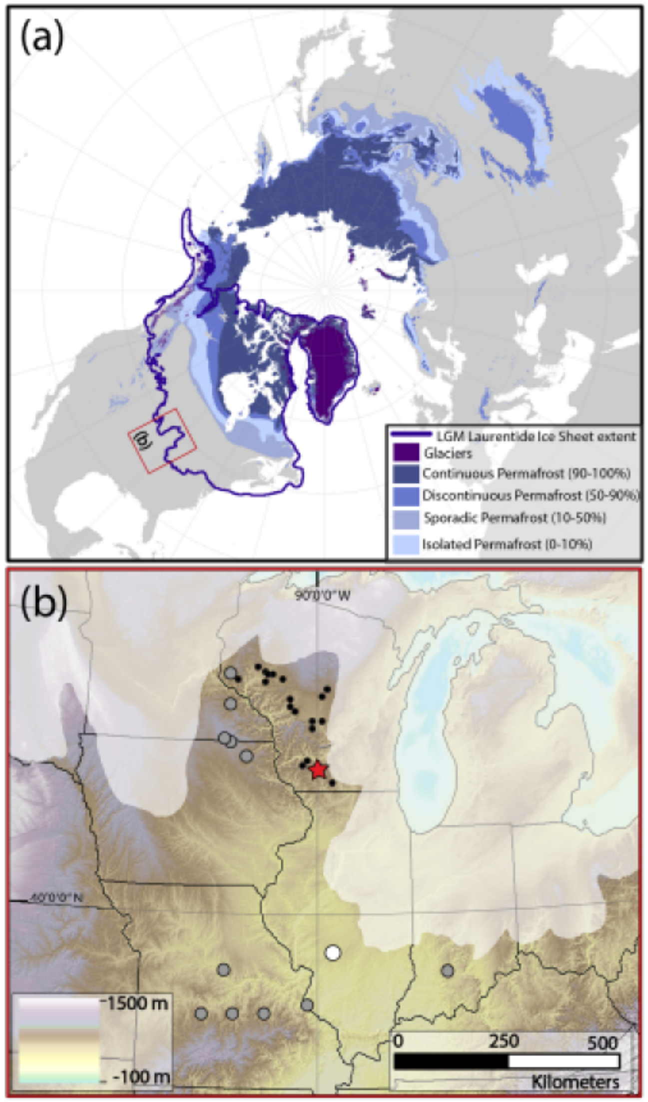

Figure 1. (a) Map of modern Northern Hemisphere permafrost zones (data from Brown et al. 2001) and the former extent of the Laurentide Ice Sheet (LIS; blue line; data from Dyke et al., 2002) at the last glacial maximum (LGM) with the regional field area for this study outlined (red box). (b) Digital elevation map of the upper midwest of the United States with the maximum extent of the LIS at the LGM overlain (white shaded region). Cave of the Mounds (red star) is located <20 km from the prior LIS margin and proximal to several geomorphic features of paleo-permafrost including ice-wedge casts and polygons (black dots). Larger circles denote locations of the Midwestern caves (gray) and lake sediment record (white) discussed in text.

frame. As a result, little climatic information on multimillennial time scales (>10^5 year) is currently available for the midcontinent of North America, specifically prior to the last glacial period. Our understanding of how paleo-permafrost conditions varied though time, therefore, is incomplete. One approach to assessing past permafrost conditions is by dating growth/no-growth intervals of cave carbonates (Vaks et al., 2013), which exist across large areas of North America (Culver et al., 1999).

1.1. Cave Records of Paleo-Permafrost

Cave carbonates, known as speleothems (Moore, 1952), are invaluable resources for investigating past climate and environmental changes because their growth requires water (Fairchild et al., 2006). They can also be precisely dated (<1% absolute age error) using U-Th geochronology methods back to 600 ka (Cheng et al., 2013; Edwards et al., 1987). A hiatus in speleothem growth can occur in response to a lack of water from aridity (Denniston et al., 2007), vegetation or environmental changes that affect carbonate saturation in groundwater (Dreybrodt, 1999), inundation by water (Polyak et al., 2018), or frozen ground (Vaks et al., 2013). Permafrost is ultimately a geological expression of climate, defined as ground that is below 0 °C for 2 years or more (French, 2017). Caves that underlie landscapes previously covered by frozen ground have the potential to record past permafrost conditions (Fankhauser et al., 2016;Lauriol et al., 1997 ; Vaks et al., 2013) because speleothem deposition requires liquid water and, thus, temperatures above freezing. Prior studies have used speleothems to reconstruct paleo-permafrost conditions from high-latitude locations (>50°) and interpret permafrost thaw when speleothems resume growth during interglacial periods (Lauriol et al., 1997; Vaks et al., 2013). In contrast, this study reconstructs the existence and duration of paleo-permafrost conditions at midlatitudes during glacial periods.

1.2. Cave of the Mounds

Cave of the Mounds (COM; 43.0°N, 89.8°W, 415 m a.s.l; Figure 1b, red star) is adjacent to Blue Mounds State Park in southwestern Wisconsin and consists of >300 m of natural passages within 10 m of the ground surface. This area of southwestern Wisconsin has remained unglaciated throughout several glacial periods of the Late Pleistocene (Figure 1b) and, thus, is referred to as the "Driftless Area" (Clayton et al., 2001). Cave of the Mounds is located 18 km from the terminal moraine of the Laurentide Ice Sheet (LIS; Dyke et al., 2002) in the Driftless Area and lies within an ice-marginal zone of geomorphic relicts of well-developed paleo-permafrost that are dated to the last glacial maximum (LGM; Figure 1b, black circles; Clayton et al., 2001). The presence of these features suggests the mean annual surface air temperature of Wisconsin during past glacial periods was below freezing for extended periods of time to allow for the ground to freeze and permafrost to form (French, 2017). We therefore infer that because COM is located within the zone of permafrost for portions of the last—and possibly earlier—glaciations, hiatuses in growth of COM speleothems during glacial periods of the late Pleistocene likely reflect temporally continuous permafrost conditions. To strengthen this interpretation and account for the possibility of local-scale controls on COM speleothem growth, we add regional context by compiling more than 300 published U-Th ages from twelve additional caves (Figure 1b, gray circles) located between 38°N and 45°N in midlatitude North America (upper Midwest). Together with our new COM U-Th ages, this compilation provides insight on the spatial and temporal extents of midcontinent paleo-permafrost during the LGM and penultimate glaciation.

2. Materials and Methods

Only carbonate stalagmites ($n = 12$) and flowstones ($n = 7$) were collected for this research because they are most likely to record stratigraphically consistent ages. Most ($n = 15$) samples collected were already dislodged and found in or very close to their original depositional positions (Figure S1 in the supporting information). When possible, speleothems were sawed parallel to their longest growth axis then polished with progressive grits of diamond-embedded pads to expose growth layers. Four of the seven flowstone samples are individual chips, approximately 1 × 1 cm in size that were removed mechanically from flowstone walls inside the cave. For U-Th geochronology, subsamples of 50 mg of calcite powder ($n = 153$) were drilled parallel to individual growth layers, including the innermost and outermost layers from each sample to capture entire growth histories. The powdered samples were then dissolved and eluted through U and Th cation and anion exchange chromatography columns that include iron coprecipitation using titration and column chemistry techniques (Edwards et al., 1987).

Final U-Th ages (datum = A.D. 1950; supporting information) were collected using a Thermo-Scientific Neptune, which is a multicollector inductively coupled plasma mass spectrometer (MC-ICP-MS) at the University of Minnesota. All uncertainties are reported as 2σ. U-decay constants (λ_{238}, λ_{234}, λ_{230}) were defined as 1.55125×10^{-10} (Jaffey et al., 1971), 2.82206×10^{-6} (Cheng et al., 2013), and 9.1705×10^{-6} (Cheng et al., 2013). Corrected ^{230}Th ages assume the initial ^{230}Th/^{232}Th atomic ratio of $4.4 \pm 2.2 \times 10^{-6}$. This is the value for a material at secular equilibrium—the error is arbitrarily assumed to be 50%—with the bulk earth ^{232}Th/^{238}U ratio of 3.8. Ages were rejected ($n = 12$) as a result of drilling difficulties (i.e., contamination), being out of stratigraphic order, or having age errors >10%. The rejected ages are not presented in figures or included in the count of total ages ($n = 141$) but are tabulated in Supporting information Data Set S1.

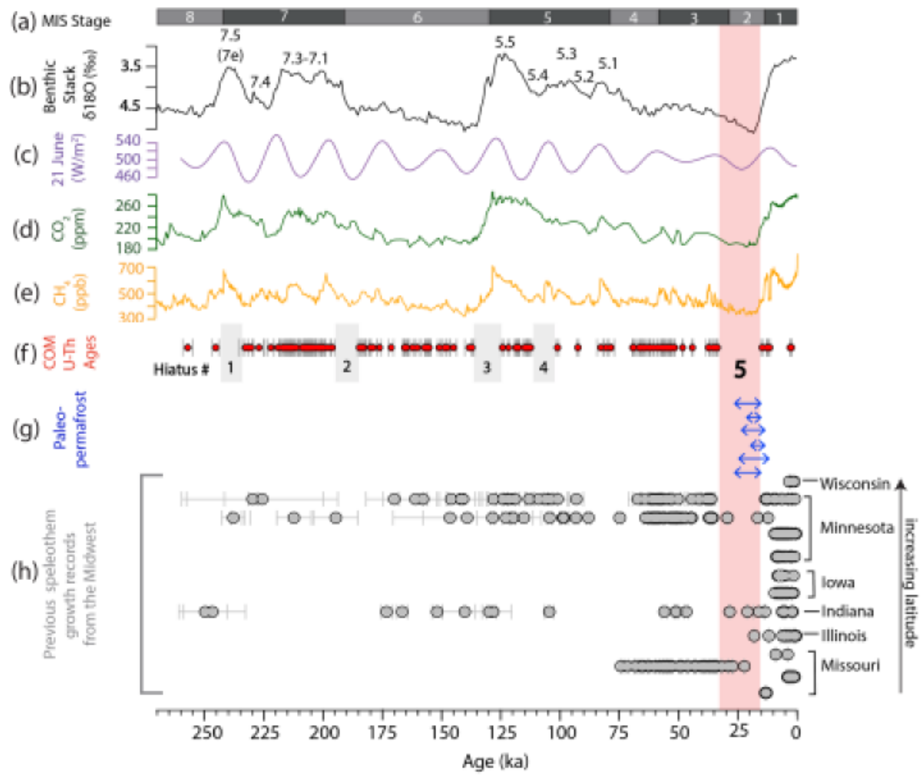

Figure 2. Speleothem U-Th ages at Cave of the Mounds (COM) in context with regional and global paleoclimate records. (a) MIS boundaries, with odd numbers signifying interglacial periods and even numbers signifying glacial periods. (b) Stacked records of $\delta^{18}O$ (‰) from benthic marine foraminifera annotated with MIS substage names (Lisiecki & Raymo, 2005). (c) Summer insolation (21 June at 43°N). (d) Atmospheric CO_2 (ppm;Bereiter et al., 2015) and (e) CH_4 (ppb; EPICA community member community members, 2004) concentrations. (f) U-Th ages from COM speleothems with associated 2σ uncertainties (this study) and statistically significant growth hiatuses (gray and red vertical bars). (g) Paleo-permafrost reconstructions based on geomorphic features in Wisconsin, including ice wedge casts and polygons (Clayton et al., 2001). (h) U-Th dates of speleothems from caves in the Midwestern United States in order of decreasing latitudeReferences provided in the main text. MIS = Marine Isotope Stage.

3. U-Th Speleothem Ages at Cave of the Mounds

We generated 141 U-Th ages (Figure 2f) from 17 speleothems (Figure S1) to determine the timing of speleothem growth at COM over the last two glacial cycles. The two oldest dates in this study are from the same growth interval and occur during Marine Isotope Stage (MIS) 8 at 257.6 ± 2.2 ka and 245.7 ± 1.3 ka, while the youngest age is from MIS 1 at 2.1 ± 0.1 ka. Overall, ages cluster primarily in interglacials, but we note growth also occurred during glacial periods (Figure 2).

To determine periods of time when environmental conditions prohibited calcite to accumulate at COM (depositional hiatuses), we first manually identified occurrences when no speleothem samples at COM were precipitating. This entailed identifying gaps in our compiled growth record that were bound by the oldest and youngest U-Th age from two separate speleothems or by two U-Th ages measured in a single speleothem that were immediately adjacent (<1 mm) to one another and separated by >10,000 years. We then created an automated Monte Carlo-based test that determined whether the lengths of these gaps (hiatuses) were statistically significant (***p*** value < 0.05). The null hypothesis for the test is that ages are distributed randomly across our finite number of speleothem samples. The Monte Carlo analysis was divided into 24 subsections that represent the seventeen individual speleothem samples collected from COM; the four speleothems that contained >50,000-year gaps in their measured ages were each divided into two subsections (Table S2). For each subsection, a uniform distribution function was used to generate a set of nonrepeating integers (i.e., ages) between the actual U-Th ages (rounded to the nearest thousand year) measured at its top and bottom. Integers were randomly selected until the size of the test set matched the number of U-Th measurements in that subsection. This random sampling was iterated 100 times per subsection and compiled in a summary matrix. For each Monte Carlo iteration, a total of only 131 integers (ages, not including duplicates) were picked across the 24 subsections; integers were not picked for replicate U-Th ages (n = 10) or for U-Th ages that were rejected by our quality control metrics (n = 12; see supporting information). Test hiatuses were calculated from the summary matrix for each iteration and were used to generate an empirical probability distribution for hiatus lengths in our sample suite. Next, p-values for rejecting the null hypothesis were calculated for a continuum of hiatus lengths (Figure S2) and are >0.05 for hiatuses of 6,200 years and longer (Figure S2, yellow star). From this automated Monte Carlo-based statistical test and our manual identification of occurrences where no calcite was precipitating in COM, we define five hiatus intervals in our speleothem growth record: 245–233 ka (Hiatus 1), 196–184 ka (Hiatus 2), 137–124 ka (Hiatus 3), 112–101 ka (Hiatus 4), and 33–15 ka (Hiatus 5; Figure 2). We note that Hiatuses 3 and 5 each overlap one of the last two glacial maxima (MISs 6 and 2, respectively) of the last 250 ka.

4. Paleo-Permafrost Conditions Across the Last Two Glacial Periods in North America

Global records, such as the benthic $\delta^{18}O$ isotope stack (Lisiecki & Raymo, 2005), suggest global ice volume was similar at the culmination of the last two glacial maxima, MISs 6 and 2. To what extent the global ice volume indicators reflect the spatial extent of individual continental ice sheets across these two glacial periods, however, is still uncertain. Prior studies found that European ice sheets were larger during MIS 6 than MIS 2 (Rohling et al., 2017), and in North America, ice extent during the Illinoian glacial phase has been reconstructed to be as or more extensive than the Wisconsin glaciation in the upper Midwest (Curry et al., 2011; Syverson & Colgan, 2004). How the local LIS spatial extent correlates with permafrost conditions in North America is also not well understood for all glaciations. The constraint on permafrost extent is well established during MIS 2 in North America based on abundant paleo-permafrost indicators and radiocarbon dating methods (Figure 2b) but less certain for MIS 6 because paleo-permafrost indicators are less geomorphologically apparent on the landscape and outside the radiocarbon dating window. Our new speleothem-based permafrost reconstruction helps clarify this uncertainty by providing proxy constraints on permafrost conditions in mid-latitude North America during both MISs 2 and 6.

We interpret the 18-kyr hiatus in the COM record from 33 to 15 ka (Hiatus 5; Figure 2) as a temporally continuous permafrost interval in southwestern Wisconsin. This interpretation is corroborated locally by other paleo-permafrost data that suggest much of the landscape of Wisconsin was covered by permafrost at this time, including radiocarbon dating of distinct permafrost relicts (e.g., ice wedge casts and polygons; Figures 1b and 2g) that formed as early as 25 ka during the LGM and thawed by approximately 14 ka (Clayton et al., 2001). The timing of thawing inferred by radiocarbon dates is similar to the COM record where there is no recorded speleothem growth after the LGM until 15 ka (Figure 2f). Likewise, regional speleothem growth records from other caves in the upper Midwest indicate no speleothem growth within 400 km of the southern terminal position of the LGM ice margin during Hiatus 5 (Figures 2h and 3c) with the exception of two dates measured at 29 and 16 ka from Minnesota (Dasgupta, 2008). This diverse and geographically dispersed compilation of proxy records supports the interpretation of a prolonged regional permafrost zone that was present in north-central North America during MIS 2.

Existing paleoclimate and speleothem growth reconstructions indicate that Hiatus 5 (MIS 2) at COM is unlikely to be related to aridity, including moisture balance reconstructions of the last glacial period from lake basins in south-central Illinois (Curry & Baker, 2000; Figure 1**b**, white dot). These records suggest precipitation rates exceeded evaporation rates from 60 to 13 ka based on multivariate analyses of pollen successions. Furthermore, the timing of these increased precipitation rates coincides with records of persistent speleothem growth at southern Midwestern caves in Indiana (Panno et al., 2016), Missouri (Denniston et al., 1999; Denniston et al., 2001; Denniston et al., 2007; Dorale et al., 1998), and Illinois (Panno et al., 2009), yet a lack of growth at northern caves in Iowa (Denniston et al., 1999; Denniston et al., 1999; Dorale et al., 1992), Minnesota (Dasgupta, 2008; Dasgupta et al., 2010; Lively, 1983), and Wisconsin (Denniston, González, Baker, et al., 1999; Figure 2h). We attribute this lack of growth at caves north of Iowa during Hiatus 5 to be a result of regional permafrost conditions.

While speleothem growth at COM during MIS 2 was nonexistent (Figures S3a–S3e), growth was prevalent in MIS 6, including six U-Th ages that record growth deep (155–137 ka) into the penultimate glacial period

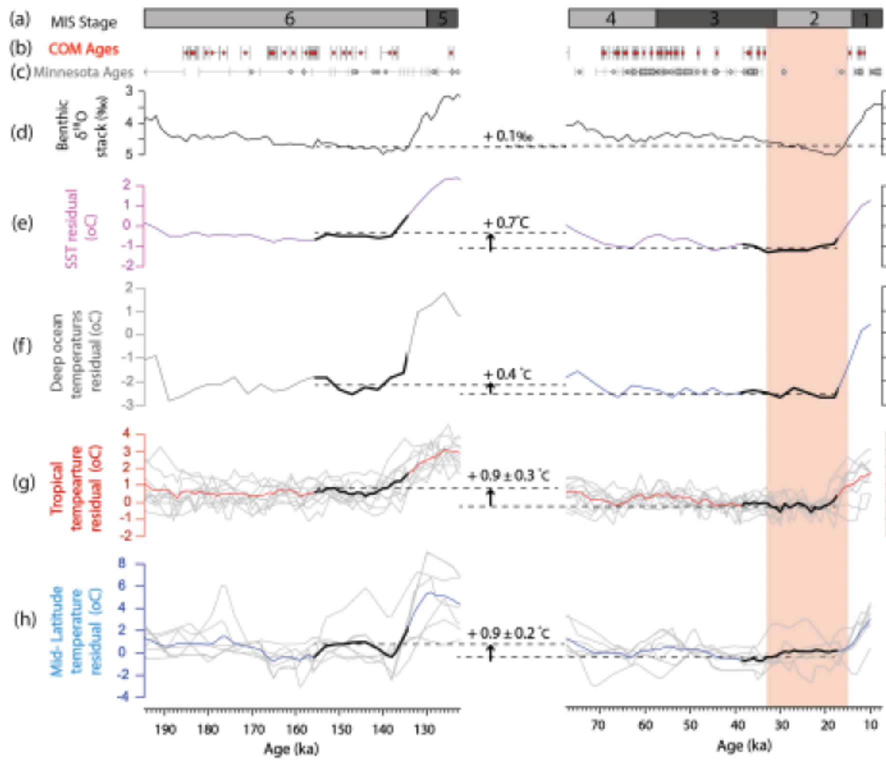

Figure 3. Paleoclimate reconstructions across MISs 6 and 2. (a) MIS as denoted by Lisiecki and Raymo (2005). (b) U-Th ages from Cave of the Mounds (this study). (c) U-Th ages from caves in Minnesota (Dasgupta, 2008; Dasgupta et al., 2010; Lively, , 1983). U-Th ages corroborate a prolonged period of permafrost conditions (red bar) during MIS 2 but not during MIS 6. (d) Benthic $\delta^{18}O$ (‰) stack from benthic marine foraminifera (Lisiecki & Raymo, 2005). (e–f) Sea surface and deep ocean temperature reconstructions relative to modern (Shakun et al., 2015). (g–h) SST reconstructions from the tropics and mid-latitudes relative to average MIS 2 temperatures. Black bolded line segments represent the time span of data used to calculate temperatures of the last 20 ka of each glacial period (155–135 ka for MIS 6 and 38–18 ka for MIS 2). Values and dashed lines in center of plot illustrate the MISs 6–2 temperature residuals in °C (references for data in supporting information Text S1). COM = Cave of the Mounds; MIS = Marine Isotope Stage; SST = sea surface temperature.

(Figures S3f–S3h). The beginning of Hiatus 3 (137–124 ka), however, overlaps with the last 5 kyr (137–132 ka) of MIS 6 as well as with Heinrich Event 11 (136–129 ka, Cheng et al., 2006; 130–129 ka, Meier et al., 2014; ~130 ka, Obrochta et al., 2014). We therefore suggest that permafrost conditions at COM were a likely cause for the beginning of Hiatus 3, but perennial frozen ground was unlikely to have persisted across the glacial termination and through the end of Hiatus 3 (124 ka). To this end, Moseley et al. (2016) summarized $\delta^{18}O$ climate proxy records from the continental United States and indicate a midpoint of the MIS 6/5 transition at ~132 ka. Speleothem growth at 128 ka from caves in Minnesota further corroborates the interpretation of earlier permafrost thawing at COM (Figure 3c; Dasgupta, 2008; Lively, 1983). As with interglacial Hiatuses 1, 2, and 4 (Figure 2), the continuation of Hiatus 3 into the last interglacial (MIS 5) could be caused by either undersampling of U-Th ages, or, more likely, local aridity or vegetation effects; speleothem deposits from regional cave records do not share these hiatuses. Thus, based on the speleothem ages at COM and the compiled U-Th speleothem growth record from the upper Midwest, we conclude that paleo-permafrost conditions endured for less time in midlatitude North America during the penultimate glacial period as compared to the last glacial.

To assess our regional interpretation in a broader context, we compiled sea surface temperature (SST) reconstructions from 46°S–50°N latitude that span the past two glacial periods (Figures 3g and 3h). We note the use of this compilation was to allow for an assessment of the relationship between large-scale temperature differences and permafrost conditions during the last two glacial periods. The SST records indicate that the average temperatures for these latitudes were 0.9 °C ± 0.2 °C warmer during the culmination of MIS 6 (155–135 ka) compared to the culmination of MIS 2 (38–18 ka; Figures 3g and 3h and Table S1).

Notably, each individual Mg/Ca SST reconstruction from the tropics demonstrates warmer temperatures during MIS 6 than during MIS 2, as do all but one of the Mg/Ca- and U^{K}_{37}-based measurements in the midlatitudes (Figure S4 and Table S1). While warmer MIS 6 SST temperatures relative to MIS 2 agree well with our paleo-permafrost reconstruction at COM, it is important to note that the $\delta^{18}O$ benthic stack (Lisiecki & Raymo, 2005; Figures 2b and 3d) and greenhouse gas concentrations (Bereiter et al., 2015; EPICA community members, 2004; Figures 2d and 2e) are nearly indistinguishable during the last two glacial periods. This observation highlights, as other studies have suggested (Rohling et al., 2017) that globally integrated climate reconstructions are important but do not illuminate regional and hemispheric heterogeneities across glacial-interglacial cycles. Based on our paleo-permafrost reconstruction, terrestrial carbon storage in North American permafrost could partly account for the diminished atmospheric greenhouse gas concentrations during MIS 2, but North American permafrost likely played a lesser role in the equally reduced greenhouse gas concentrations during the culmination of MIS 6.

5. Conclusions

Our new record of speleothem growth at COM combined with the compilation from regional caves provides new insight into permafrost and climate conditions during the last two glacial periods of the late Pleistocene. These records indicate a shorter interval of permafrost and warmer conditions in the late stages of MIS 6 as compared to MIS 2 in midlatitude North America. Based on our composite SST reconstructions, warmer MIS 6 conditions appear to occur throughout middle and tropical latitudes. Together, these results demonstrate that permafrost conditions in North America and global temperatures varied between the last two glacial periods, despite global-scale climate indicators (Bereiter et al., 2015; EPICA community members, 2004; Lisiecki & Raymo, 2005; Shakun et al., 2015) that suggest relatively consistent climate and atmospheric greenhouse gas conditions.

Acknowledgments
This work was supported by the University of Wisconsin-Madison (S. A. M.), the Center for Climatic Research (I. J. O.), the Geologic Society of America (C. J. B.), and the National Science Foundation (P2C2-1805629 to S. A. M. and I. J. O.). We thank J. Klimczak and A. Wescott for their permission to collect samples at Cave of the Mounds. Samples analyzed in this study are curated at the University of Wisconsin-Madison Geology Museum. All speleothem U-Th data and SST reconstructions compiled for this study are entirely contained within the paper and references and are available at the National Center for Environmental Information.

References

Bereiter, B., Eggleston, S., Schmitt, J., Nehrbass-Ahles, C., Stocker, T. F., Fischer, H., et al. (2015). Revision of the EPICA Dome C CO_2 record from 800 to 600 kyr before present. *Geophysical Research Letters*, *42*, 542–549. https://doi.org/10.1002/2014GL061957

Budyko, M. I. (1969). The effect of solar radiation variations on the climate of the earth. *Tellus*, *21*(5), 611–619.

Cheng, H., Edwards, R. L., Shen, C.-C., Polyak, V. J., Asmerom, Y., Woodhead, J., et al. (2013). Improvements in ^{230}Th dating, ^{230}Th and ^{234}U half-life values, and U-Th isotopic measurements by multi-collector inductively coupled plasma mass spectrometry. *Earth and Planetary Science Letters*, *371*, 82–91.

Cheng, H., Edwards, R. L., Wang, Y., Kong, X., Ming, Y., Kelly, M. J., et al. (2006). A penultimate glacial monsoon record from Hulu Cave and two-phase glacial terminations. *Geology*, *34*(3), 217–220. https://doi.org/10.1130/G22289.1

Clayton, L., Attig, J. W., & Mickelson, D. M. (2001). Effects of late Pleistocene permafrost on the landscape of Wisconsin, USA. *Boreas*, *30*(3), 173–188.

Culver, D. C., Hobbs, H. H. III, Christman, M. C., & Master, L. L. (1999). Distribution map of caves and cave animals in the United States. *Journal of Cave and Karst Studies*, *61*(3), 139–140.

Curry, B. B., & Baker, R. G. (2000). Paleohydrology, vegetation, and climate during the last interglaciation (Sangamon Episode) in south-central Illinois. *Palaeogeography Palaeoclimatology Palaeoecology*, *155*, 59–81. https://doi.org/10.1016/S0031-0182(99)00094-2

Curry, B. B., Grimley, D. A., & McKay, E. D. III (2011). Quaternary glaciations in Illinois. In *Developments in Quaternary Sciences*, (Vol. 15, pp. 467–487). Amsterdam: Elsevier.

Dasgupta, S. (2008). *High-resolution speleothem record of late Quaternary climate change from the Upper Midwest, USA*. Minneapolis: University of Minnesota.

Dasgupta, S., Saar, M. O., Edwards, R. L., Shen, C.-C., Cheng, H., & Alexander, E. C. Jr. (2010). Three thousand years of extreme rainfall events recorded in stalagmites from Spring Valley Caverns, Minnesota. *Earth and Planetary Science Letters*, *300*(1–2), 46–54.

Denniston, R. F., DuPree, M., Dorale, J. A., Asmerom, Y., Polyak, V. J., & Carpenter, S. J. (2007). Episodes of late Holocene aridity recorded by stalagmites from Devil's Icebox Cave, central Missouri, USA. *Quaternary Research*, *68*(1), 45–52. https://doi.org/10.1016/j.yqres.2007.04.001

Denniston, R. F., González, L. A., Asmerom, Y., Baker, R. G., Reagan, M. K., & Bettis, E. A. (1999). Evidence for increased cool season moisture during the middle Holocene. *Geology*, *27*(9), 815–818.

Denniston, R. F., González, L. A., Asmerom, Y., Polyak, V., Reagan, M. K., & Saltzman, M. R. (2001). A high-resolution speleothem record of climatic variability at the Allerød-Younger Dryas transition in Missouri, central United States. *Palaeogeography, Palaeoclimatology, Palaeoecology*, *176*, 147–155. https://doi.org/10.1016/S0031-0182(01)00334-0

Denniston, R. F., González, L. A., Baker, R. G., Asmerom, Y., Reagan, M. K., Edwards, R. L., & Alexander, E. C. (1999). Speleothem evidence for Holocene fluctuations of the prairie-forest ecotone, north-central USA. *The Holocene*, *9*(6), 671–676.

Denniston, R. F., González, L. A., Semken, H. A., Asmerom, Y., Baker, R. G., Recelli-Snyder, H., et al. (1999). Integrating stalagmite, vertebrate, and pollen sequences to investigate Holocene vegetation and climate change in the southern Midwestern United States. *Quaternary Research*, *52*(3), 381–387. https://doi.org/10.1006/qres.1999.2075

Dorale, J. A., Edwards, R. L., Ito, E., & González, L. A. (1998). Climate and vegetation history of the midcontinent from 75 to 25 ka: A speleothem record from Crevice Cave, Missouri, USA. *Science*, *282*(5395), 1871–1874.

Dorale, J. A., González, L. A., Reagan, M. K., Pickett, D. A., Murrell, M. T., & Baker, R. G. (1992). A high-resolution record of Holocene climate change in speleothem calcite from Cold Water Cave, northeast Iowa. *Science*, *258*(5088), 1626–1631.

Dreybrodt, W. (1999). Chemical kinetics, speleothem growth and climate. *Boreas*, *28*(3), 347–356.
Dyke, A. S., Andrews, J. T., Clark, P. U., England, J. H., Miller, G. H., Shaw, J., & Veillette, J. J. (2002). The Laurentide and Innuitian ice sheets during the last glacial maximum. *Quaternary Science Reviews*, *21*(1–3), 9–31. https://doi.org/10.1016/S0277-3791(01)00095-6
Edwards, R. L., Chen, J. H., & Wasserburg, G. J. (1987). $^{238}U^{234}U^{230}Th^{232}Th$ systematics and the precise measurement of time over the past 500,000 years. *Earth and Planetary Science Letters*, *81*(2–3), 175–192.
EPICA community members (2004). Eight glacial cycles from an Antarctic ice core. *Nature*, *429*, 623–628.
Fairchild, I. J., Smith, C. L., Baker, A., Fuller, L., Spötl, C., Mattey, D., & McDermott, F. (2006). Modification and preservation of environmental signals in speleothems. *Earth-Science Reviews*, *75*(1), 105–153.
Fankhauser, A., McDermott, F., & Fleitmann, D. (2016). Episodic speleothem deposition tracks the terrestrial impact of millennial-scale last glacial climate variability in SW Ireland. *Quaternary Science Reviews*, *152*, 104–117.
French, H. M. (2017). *The periglacial environment*. New York: John Wiley & Sons.
Grosse, G., Romanovsky, V., Jorgenson, T., Anthony, K. W., Brown, J., & Overduin, P. P. (2011). Vulnerability and feedbacks of permafrost to climate change. *Eos, Transactions American Geophysical Union*, *92*(9), 73–74.
Hays, J. D., Imbrie, J., & Shackleton, N. J. (1976). Variations in the Earth's orbit: Pacemaker of the ice ages. *Science*, *194*, 1121–1132.
Heimann, M., & Reichstein, M. (2008). Terrestrial ecosystem carbon dynamics and climate feedbacks. *Nature*, *451*(7176), 289–292.
Hope, C., & Schaefer, K. (2016). Economic impacts of carbon dioxide and methane released from thawing permafrost. *Nature Climate Change*, *6*(1), 56–59.
Jaffey, A. H., Flynn, K. F., Glendenin, L. E., Bentley, W. t., & Essling, A. M. (1971). Precision measurement of half-lives and specific activities of ^{235}U and ^{238}U. *Physical Review C*, *4*(5), 1889–1906. https://doi.org/10.1103/PhysRevC.4.1889
Lauriol, B., Ford, D. C., Cinq-Mars, J., & Morris, W. A. (1997). The chronology of speleothem deposition in northern Yukon and its relationships to permafrost. *Canadian Journal of Earth Sciences*, *34*(7), 902–911.
Lisiecki, L. E., & Raymo, M. E. (2005). A Pliocene-Pleistocene stack of 57 globally distributed benthic $\delta^{18}O$ records. *Paleoceanography*, *20*, PA1003. https://doi.org/10.1029/2004pa001071
Lively, R. S. (1983). Late Quaternary U-series speleothem growth record from southeastern Minnesota. *Geology*, *11*(5), 259–262.
Meier, K. J. S., Berger, C., & Kinkel, H. (2014). Increasing coccolith calcification during CO_2 rise of the penultimate deglaciation (Termination II). *Marine Micropaleontology*, *112*, 1–12.
Moore, G. W. (1952). Speleothem—A new cave term. *National Speleological Society News*, *10*(6), 2–2.
Moseley, G. E., Edwards, R. L., Wendt, K. A., Cheng, H., Dublyansky, Y., Lu, Y., et al. (2016). Reconciliation of the Devils Hole climate record with orbital forcing. *Science*, *351*(6269), 165–168.
Obrochta, S. P., Crowley, T. J., Channell, J. E., Hodell, D. A., Baker, P. A., Seki, A., & Yokoyama, Y. (2014). Climate variability and ice-sheet dynamics during the last three glaciations. *Earth and Planetary Science Letters*, *406*, 198–212.
Panno, S. V., Chirienco, M. I., Bauer, R. A., Lundstrom, C. C., Zhang, Z., & Hackley, K. C. (2016). Possible earthquakes recorded in Stalagmites from a cave in South-Central Indiana. *Bulletin of the Seismological Society of America*, *106*(5), 2364–2375.
Panno, S. V., Lundstrom, C. C., Hackley, K. C., Curry, B. B., Fouke, B. W., & Zhang, Z. (2009). Major earthquakes recorded by speleothems in Midwestern US caves. *Bulletin of the Seismological Society of America*, *99*(4), 2147–2154.
Polyak, V. J., Onac, B. P., Fornós, J. J., Hay, C., Asmerom, Y., Dorale, J. A., et al. (2018). A highly resolved record of relative sea level in the western Mediterranean Sea during the last interglacial period. *Nature Geoscience*, *11*(11), 860–864. https://doi.org/10.1038/s41561-018-0222-5
Rohling, E. J., Hibbert, F. D., Williams, F. H., Grant, K. M., Marino, G., Foster, G. L., et al. (2017). Differences between the last two glacial maxima and implications for ice-sheet, $\delta^{18}O$, and sea-level reconstructions. *Quaternary Science Reviews*, *176*, 1–28. https://doi.org/10.1016/j.quascirev.2017.09.009
Sellers, W. D. (1969). A global climatic model based on the energy balance of the earth-atmosphere system. *Journal of Applied Meteorology*, *8*(3), 392–400.
Shakun, J. D., Lea, D. W., Lisiecki, L. E., & Raymo, M. E. (2015). An 800-kyr record of global surface ocean $\delta^{18}O$ and implications for ice volume-temperature coupling. *Earth and Planetary Science Letters*, *426*, 58–68.
Smith, S. L., Romanovsky, V. E., Lewkowicz, A. G., Burn, C. R., Allard, M., Clow, G. D., et al. (2010). Thermal state of permafrost in North America: A contribution to the international polar year. *Permafrost and Periglacial Processes*, *21*(2), 117–135. https://doi.org/10.1002/ppp.690
Syverson, K. M., & Colgan, P. M. (2004). The Quaternary of Wisconsin: A review of stratigraphy and glaciation history. In *Developments in quaternary sciences*, (Vol. 2, pp. 295–311). New York: Elsevier.
Vaks, A., Gutareva, O. S., Breitenbach, S. F., Avirmed, E., Mason, A. J., Thomas, A. L., et al. (2013). Speleothems reveal 500,000-year history of Siberian permafrost. *Science*, *340*(6129), 183–186. https://doi.org/10.1126/science.1228729
Zimov, S. A., Schuur, E. A., & Chapin, F. S. (2006). Permafrost and the global carbon budget. *Science*, *312*(5780), 1612–1613.

References From the Supporting Information

Bard, E., & Rickaby, R. E. (2009). Migration of the subtropical front as a modulator of glacial climate. *Nature*, *460*(7253), 380–383. https://doi.org/10.1038/nature08189
Herbert, T. D., Peterson, L. C., Lawrence, K. T., & Liu, Z. (2010). Tropical ocean temperatures over the past 3.5 million years. *Science*, *328*(5985), 1530–1534.
Lea, D. W., Pak, D. K., & Spero, H. J. (2000). Climate impact of late Quaternary equatorial Pacific sea surface temperature variations. *Science*, *289*(5485), 1719–1724.
Martínez-Garcia, A., Rosell-Melé, A., McClymont, E. L., Gersonde, R., & Haug, G. H. (2010). Subpolar link to the emergence of the modern equatorial Pacific cold tongue. *Science*, *328*(5985), 1550–1553.
Mashiotta, T. A., Lea, D. W., & Spero, H. J. (1999). Glacial-interglacial changes in subantarctic sea surface temperature and $\delta^{18}O$-water using foraminiferal Mg. *Earth and Planetary Science Letters*, *170*(4), 417–432.
Medina-Elizalde, M., & Lea, D. W. (2005). The mid-Pleistocene transition in the tropical Pacific. *Science*, *310*(5750), 1009–1012.
Nürnberg, D., Müller, A., & Schneider, R. R. (2000). Paleo-sea surface temperature calculations in the equatorial east Atlantic from Mg/Ca ratios in planktic foraminifera: A comparison to sea surface temperature estimates from $U_{37}^{K'}$, oxygen isotopes, and foraminiferal transfer function. *Paleoceanography and Paleoclimatology*, *15*(1), 124–134.

Nürnberg, D., Ziegler, M., Karas, C., Tiedemann, R., & Schmidt, M. W. (2008). Interacting loop current variability and Mississippi River discharge over the past 400 kyr. *Earth and Planetary Science Letters*, *272*(1–2), 278–289.
Pahnke, K., Zahn, R., Elderfield, H., & Schulz, M. (2003). 340,000-year centennial-scale marine record of Southern Hemisphere climatic oscillation. *Science*, *301*(5635), 948–952.
Pelejero, C., Calvo, E., Barrows, T. T., Logan, G. A., & De Deckker, P. (2006). South Tasman Sea alkenone palaeothermometry over the last four glacial/interglacial cycles. *Marine Geology*, *230*(1–2), 73–86.
Pena, L. D., Cacho, I., Ferretti, P., & Hall, M. A. (2008). El Niño–Southern Oscillation-like variability during glacial terminations and interlatitudinal teleconnections. *Paleoceanography*, *23*, PA3101. https://doi.org/10.1029/2008PA001620
Russon, T., Elliot, M., Sadekov, A., Cabioch, G., Corrège, T., & De Deckker, P. (2011). The mid-Pleistocene transition in the subtropical southwest Pacific. *Paleoceanography*, *26*, PA1211. https://doi.org/10.1029/2010PA002019
Schmidt, M. W., Vautravers, M. J., & Spero, H. J. (2006). Western Caribbean Sea surface temperatures during the late Quaternary. *Geochemistry, Geophysics, Geosystems*, *7*, Q02P10. https://doi.org/10.1029/2005GC000957